Traffic & Transportation

Transportation Route Optimisation Method for Agricultural Product Logistics Based on TSVNS

Hongyan DONG[1]

Original Scientific Paper
Submitted: 17 Feb 2025
Accepted: 22 Sep 2025
Published: 28 Apr 2026

[1] donghongyan2024@163.com, College of Cultural Creativity and Tourism, Yuncheng Vocational and Technical University, Yuncheng, China

Publisher:
Faculty of Transport and Traffic Sciences, University of Zagreb

ABSTRACT
As the demand for agricultural product logistics grows rapidly and requirements for timeliness and freshness in cold chain transportation increase, existing vehicle route optimisation methods face challenges in addressing multi-objective conflicts and dynamic environmental changes. To address these issues, the study proposes a hybrid optimisation algorithm based on tabu search and variable neighbourhood search, combined with a logistics route method incorporating non-dominated sorting genetic algorithm, and designs a transportation route model for agricultural product logistics vehicles suitable for cold chain transportation. Experimental results of logistics route planning show that the proposed model generates 8 paths, significantly fewer than the comparison models. A real-world scenario validation under different temperature conditions shows that as the temperature difference increases from 5°C to 45°C, the cargo loss increases from 365.32 yuan to 552.93 yuan, and the refrigeration cost also gradually increases. Other indicators similarly rise with the increasing temperature difference, and the total distribution cost reaches 7,069.73 RMB. The experimental results indicate that the proposed route optimisation model can be applied to agricultural product logistics scenarios with complex constraints and is of significant importance for improving cold chain transportation efficiency, reducing logistics costs and ensuring agricultural product quality.

KEYWORDS
agricultural product logistics; vehicle route optimisation; tabu search; variable neighbourhood search; multi-objective optimisation.

1. INTRODUCTION

With the rapid development of e-commerce and modern logistics, agricultural product logistics plays a crucial role in ensuring the efficient operation of the food supply chain. Particularly in the cold chain logistics field, agricultural products are highly sensitive to temperature control and delivery timeliness [1]. Traditional route optimisation typically involves linear programming and integer programming, where mathematical models are established to seek optimal solutions [2, 3]. However, traditional methods are insufficient in handling multi-objective problems and lack flexibility. When the problem scale increases, the computational load of traditional methods increases sharply. With the development of technology, current methods focus on more complex algorithms such as particle swarm optimisation (PSO), genetic algorithm (GA), simulated annealing (SA) and tabu search (TS), which can effectively address large-scale nonlinear optimisation problems, especially in cold chain logistics, where factors like product shelf life, temperature control and time window constraints need to be considered [4, 5]. For example, Azarkish et al. addressed the uncertainty in the multi-depot electric vehicle routing problem by proposing a fuzzy bi-objective mathematical model. Experimental results showed that the model and algorithm provided an efficient solution for green logistics route optimisation [6]. Liu B et al. proposed a new algorithm based on a task-time graph to optimise the path

for drone-based joint cargo delivery and on-site sensing. Experimental results indicated that this method improved task rewards by more than 18% compared to alternative solutions [7]. However, as the conditions in logistics routes become increasingly complex, the focus of current research is on how to optimise transportation routes, reduce logistics costs and lower carbon emissions while meeting cold chain constraints.

Agricultural product logistics route optimisation needs to consider not only economic benefits but also ensure the freshness and quality of the products, with an emphasis on time efficiency, cost efficiency and temperature control. It is necessary to integrate multi-objective optimisation to improve the overall efficiency and responsiveness of the supply chain [8]. For example, Liu Y et al. addressed the challenges of improving time efficiency, economic costs, safety and network security in modern logistics networks by providing a comprehensive survey on the current status and potential applications of artificial intelligence in intelligent logistics network physical systems [9]. Wu et al. proposed a multi-objective scheduling model for cold chain logistics based on multi-source data association. In real-world transportation data tests in Guangzhou and Shenzhen, the method outperformed six recently advanced multi-objective optimisation algorithms in three-objective optimisation [10]. However, the methods used in current research often have shortcomings in modelling complex constraints, making it difficult to comprehensively optimise the balance between cost, time and freshness. TS is a local search-based optimisation algorithm that avoids revisiting previously explored solutions by maintaining a taboo list. This helps the search process escape from local optima and explore a broader solution space [11]. In cold chain logistics optimisation, TS can effectively handle multi-objective optimisation problems, such as minimising costs while maximising service levels [12]. Variable neighbourhood search (VNS) is a method that systematically changes the neighbourhood structure to find the global optimal solution in different neighbourhoods [13]. VNS is particularly effective in handling multiple paths and time window issues in cold chain logistics. Moreover, in practical applications, VNS is less sensitive to parameters and is easy to implement and adjust [14]. The second-generation non-dominated sorting genetic algorithm (NSGA-II) is a popular multi-objective optimisation algorithm commonly used to solve complex problems that require optimising multiple conflicting objectives simultaneously [15]. For the agricultural product logistics vehicle route optimisation problem, this study proposes an improved hybrid algorithm that combines TS and VNS, and integrates it with the NSGA-II algorithm to construct a dynamic hybrid optimisation model for the agricultural cold chain logistics vehicle routing problem, based on dynamic hybrid optimisation for the agricultural cold chain logistics vehicle routing problem using NSGA-II and TS-VNS (NSGA-TSVNS). To achieve efficient balance when handling multiple conflicting objectives, the proposed model enhances the algorithm's ability to adapt to dynamic changes in complex logistics environments. Additionally, the model dynamically adjusts the taboo list and neighbourhood structure to improve responsiveness to real-time transportation condition changes, aiming for better stability and easier deployment in actual logistics operations. This model can be widely applied to logistics and transportation problems that need to consider multiple constraints and objectives simultaneously.

2. METHOD

2.1 TSVNS for agricultural product logistics route optimisation

Agricultural products are perishable and highly sensitive to transportation conditions, so it is essential to integrate cold chain logistics technology in route optimisation to ensure product quality and freshness during transportation [16]. The advantage of VNS in agricultural logistics vehicle route planning lies in its ability to efficiently handle complex logistics route optimisation problems while also meeting the stringent requirements for timeliness and transportation environment in agricultural cold chain logistics [17, 18]. This algorithm dynamically adjusts the search neighbourhood, enabling it to quickly find the global optimal solution while solving local optimum problems, thus optimising transportation routes, reducing delivery costs and improving logistics efficiency [19]. The operating principle of VNS is shown in *Figure 1*.

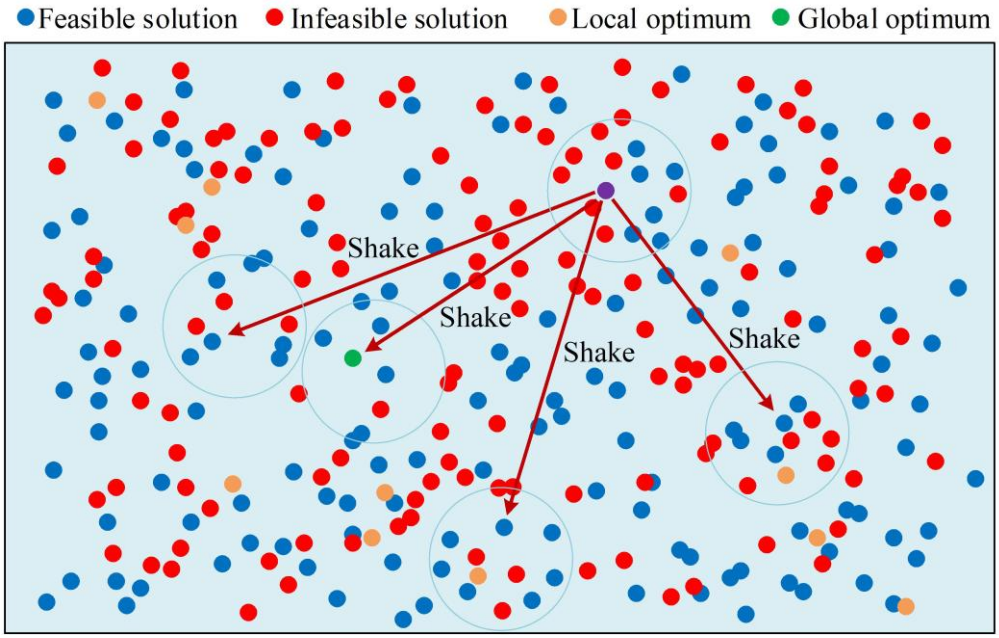

Figure 1 – Schematic diagram of VNS operation

In *Figure 1*, VNS searches for the optimal solution by continuously switching neighbourhoods in the solution space. Starting from the initial solution, it performs local search within the current neighbourhood to find an improved solution. If no improvement is found, it switches to a larger neighbourhood and uses perturbation operations to jump to a new region and restart the search, thus avoiding being trapped in a local optimum. This process is repeated until a solution that meets the conditions is found. The circles in the figure represent different neighbourhoods, while the red lines and perturbation steps indicate transitions into different regions of the solution space. The points in different colours represent the distribution of solutions. The ultimate goal of VNS is to explore the global optimal solution. Candidate solutions are generated in multiple neighbourhoods using neighbourhood search, as shown in *Equation 1*.

$$\mathrm{N}_k(X_i)=\{X'_{i,1},X'_{i,2},...,X'_{i,m}\},\quad k=1,2,...,K \tag{1}$$

In *Equation 1*, $\mathrm{N}_k(X_i)$ denotes the set of candidate solutions generated by solution X_i in the k th neighbourhood, and K denotes the total number of neighbourhoods. The expressions for logistics route exchange, node insertion, and logistics route reversal are defined for the neighbourhood, as shown in *Equation 2*.

$$\begin{cases} X'_{swap}=Swap(X_i,i,j) \\ X'_{insert}=Insert(X_i,i,j) \\ X'_{reverse}=\mathrm{Re}verse(X_i,i,j) \end{cases} \tag{2}$$

In *Equation 2*, $Swap(X_i,i,j)$ means swapping the two customers at positions i and j in solution X_i; $Insert(X_i,i,j)$ means inserting the customer at position i into position j; $\mathrm{Re}verse(X_i,i,j)$ means reversing the customer sequence between positions i and j in X_i. Although VNS can explore the solution space by dynamically switching neighbourhoods, it may face issues of solution search repetition and decreased efficiency in complex multi-constraint optimisation problems [20]. TS, on the other hand, can avoid redundant searches of logistics routes by recording the visited solutions and their characteristics [21, 22]. By introducing a taboo list and memory function, TS effectively compensates for the shortcomings of VNS in the application of agricultural product logistics route planning, particularly in preventing search repetition and escaping local optima [23, 24]. The operation process of TS is shown in *Figure 2*.

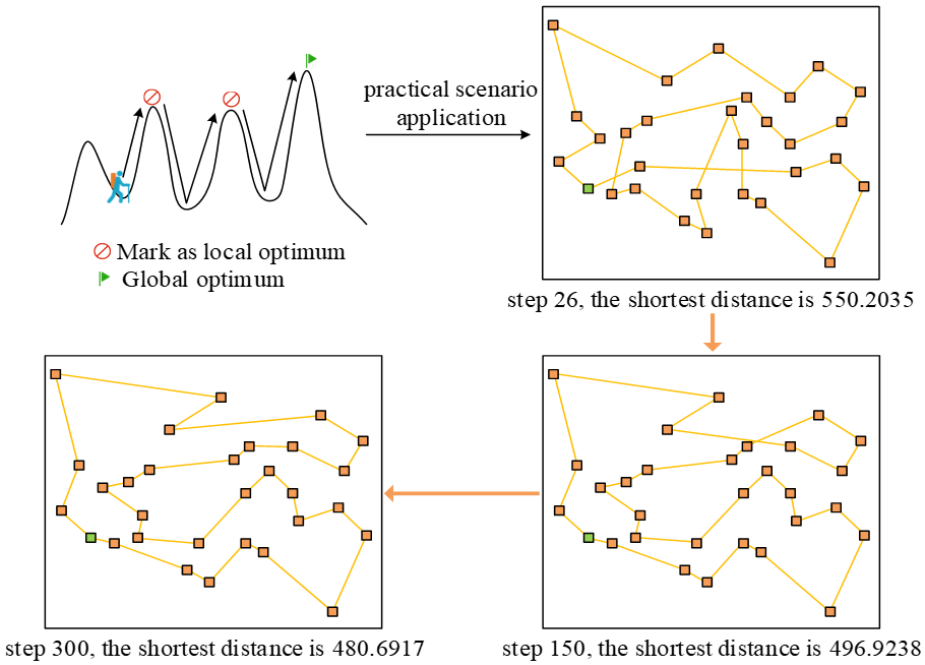

Figure 2 – Schematic diagram of the operation process of TS

This is depicted in *Figure 2*, where TS begins from the initial solution and explores its neighbourhood to identify the best candidate. If the new solution is better than the current solution and is not in the taboo list, it is updated as the current solution, and the related operations are recorded in the taboo list to avoid cycling back to previously explored solutions. The taboo list is dynamically updated to maintain its length and allows certain solutions to accept worse solutions in order to escape from local optima. The entire process iteratively searches for the global optimal solution until the stopping criteria are met, such as reaching the maximum number of iterations or the objective. The taboo list records the most recently visited solutions or operations, as shown in *Equation 3*.

$$\mathrm{T} = \{X_{tabu1}, X_{tabu2}, \ldots\} \tag{3}$$

In *Equation 3*, X_{tabu} represents the taboo solution. After each move, the new solution is added to the taboo list, and expired solutions are removed. The parameters α and β represent the adaptation rates of the neighbourhood size and the tabu list length, respectively. In the experiment, they are set to 0.5 and 0.3 to balance convergence speed and exploration diversity. Sensitivity tests confirmed stability in a ±0.1 range. Then, the neighbourhood size is adjusted, as shown in *Equation 4*.

$$N = N_0 \cdot (1 + \alpha \cdot \frac{w}{w_{total}}) \tag{4}$$

In *Equation 4*, α represents the neighbourhood size. N and N_0 represent the current neighbourhood size and the initial neighbourhood size, respectively, while w and w_{total} represent the number of iterations without improvement and the total number of iterations. Then, the length of the taboo list is adjusted, as shown in *Equation 5*.

$$T = T_0 \cdot (1 + \beta \cdot \frac{w}{w_{total}}) \tag{5}$$

In *Equation 5*, T and T_0 represent the current taboo list length and the initial taboo list length, respectively. β represents the adjustment rate for prohibited lengths. The objective values of the candidate solutions for each neighbourhood are evaluated, and the optimal solution is selected, as shown in *Equation 6*.

$$X^* = \arg \min_{X' \in \mathrm{N}_k(X_i) \setminus \mathrm{T}} Z(X') \tag{6}$$

In *Equation 6*, $Z(X^{'})$ represents the objective value vector of the candidate solutions. In the k th neighbourhood $\mathrm{N}_k(X_i)$, select the solution $X^{'}$ with the smallest objective function value among the candidate solutions that do not belong to the tabu list T, i.e. X^*. TSVNS effectively combines the memory function of the taboo list in TS with the dynamic neighbourhood switching in VNS, successfully avoiding local optima and redundant searches. This enhances the global optimisation capability and efficiency of agricultural product logistics route planning, meeting the strict requirements for timeliness and cost in cold chain logistics. The agricultural logistics route optimisation method based on TSVNS is shown in *Figure 3*.

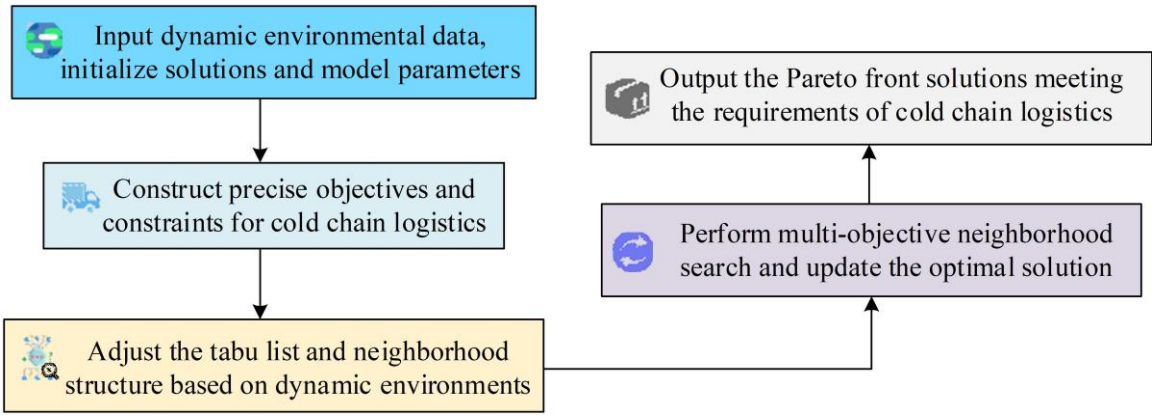

Figure 3 – TSVNS-based logistics route optimisation method for agricultural products

Figure 3 illustrates the operation process of TSVNS. Starting with the input of dynamic environmental data, the initial solution and model parameters are first initialised. Then, precise objectives and constraints for cold chain logistics are constructed to meet the problem characteristics. Next, the taboo list and neighbourhood structure are adjusted according to the dynamic environment to enhance the algorithm's adaptability. Multi-objective neighbourhood search is executed, and the optimal solution is gradually updated. Finally, the Pareto frontier solution set that meets cold chain logistics requirements is output. The entire process dynamically integrates environmental factors to optimise the logistics route scheme, balancing cold chain constraints and multi-objective performance. The impact of dynamic environmental data can be expressed through dynamic adjustment of the objective function or constraints, as shown in *Equation 7*.

$$C_{ij}(t) = C_{ij}^{0} + \Delta C_{ij}(t) \tag{7}$$

In *Equation 7*, C_{ij}^{0} represents the initial logistics route cost, and $\Delta C_{ij}(t)$ represents the real-time cost increment caused by the dynamic environment.

2.2 Agricultural product logistics transportation route model based on NSGA-TSVNS

Although TSVNS significantly enhances global search ability through dynamic neighbourhood switching and the combination of the tabu memory function, it may still struggle to balance multiple conflicting objectives, such as transportation cost, time and cold chain conditions, when solving multi-objective optimisation problems. NSGA-II, as a classic multi-objective evolutionary algorithm, offers good solution set diversity, effectively generating evenly distributed Pareto front solutions [25]. Therefore, by combining NSGA-II and TSVNS, multi-objective optimisation problems can be handled by NSGA-II in agricultural logistics route planning, while utilising TSVNS for local fine search capabilities in single-objective optimisation. This combination further improves the solution quality and overall performance in multi-objective optimisation, enabling efficient optimisation of transportation logistics routes under cold chain logistics conditions. A schematic diagram of the non-dominated sorting and crowding distance calculation process in NSGA-II is shown in *Figure 4*.

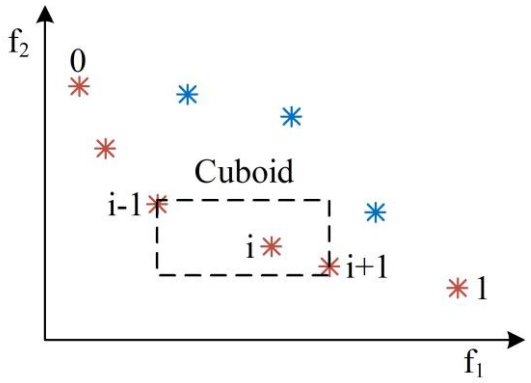

Figure 4 – Schematic diagram of the calculation process of NGSA-II

As illustrated in *Figure 4*, the solution set of NSGA-II is divided into different non-dominated fronts based on their dominance relationships. The red and blue points represent different non-dominated fronts. Within each front, the crowding distance of the solutions is calculated to measure their distribution density. Solutions with larger crowding distances are located in sparser regions, making them more likely to be selected for the next generation, thus achieving a balance between solution diversity and optimisation performance. In the NSGA-II algorithm, a population P_0 is randomly generated, with each solution X_i consisting of logistics route allocation, time and temperature control schemes. The specific expression is shown in *Equation 8*.

$$P_0 = \{X_1, X_2, ..., X_N\} \tag{8}$$

In *Equation 8*, $X_i = \{x_{ijk}, y_{ik}, t_{ik}\}$ represents the i-th solution, which includes the vehicle logistics route, delivery decisions and time allocation. For each solution X_i, the objective function value $Z(X_i) = [Z_1(X_i), Z_2(X_i), Z_3(X_i), Z_4(X_i)]$ is calculated, followed by non-dominated sorting, and the population is divided into multiple fronts, as shown in *Equation 9*.

Let :
$X_i \in P_0$
$Z(X) = [Z_1(X), Z_2(X), ..., Z_m(X)]$ be the vector of objective values
Then X dominates X (denoted) if and only if: (9)
$\forall k \in \{1, ..., m\}$, $Z_k(X_i) \le X_j$ and $\exists k \in \{1, ..., m\}$, $Z_k(X_i) < X_j$
Then the first Pareto front is given by:
$F_1 = \{X_i \in P_0 \mid \text{ó} X_j \in P_0, X_j \prec X_i\}$

In *Equation 9*, $Z_k(X_i)$ represents the value of the i-th solution on the objectives, such as transportation cost, time, etc. $F_1, F_2, ...$ is the hierarchical set of non-dominated solutions. In multi-objective optimization, if and only if solution X_i dominates solution X_j (denoted as $X_i \prec X_j$), for every objective $k \in \{1,2,...M\}, Z_k(X_i) \le Z_k(X_j)$, and there exists at least one objective $k \in \{1,2,...M\}$, such that $Z_k(X_i) < Z_k(X_j)$.

For each front Z_m, the solutions are sorted by objective values, and the crowding distance for each solution is calculated, as shown in *Equation 10*.

$$d_i = \sum_{k=1}^{M} \left(\frac{Z_k^{i+1} - Z_k^{i-1}}{Z_k^{\max} - Z_k^{\min}} \right) \tag{10}$$

In *Equation 10*, let M be the total number of objectives, and let X_i denote the current solution in the population. Z_k^{i+1} and Z_k^{i-1} represent the adjacent values of the solution on the objectives, while $Z_k^{\max}$ and $Z_k^{\min}$ are the maximum and minimum values of the objectives, respectively. Then, selection, crossover and mutation are performed, as shown in *Equation 11*.

$$\begin{cases} X_{new} = Crossover\left(X_{initial1}, X_{initial2}\right) \\ X_{mutated} = Mutation(X_{new}) \\ X_i^{(t)} \in P_t \rightarrow X_i^{crossover} \rightarrow X_i^{mutation} \in Q_t \end{cases} \quad (11)$$

In *Equation 11*, P_t represents the t-th population, $X_{initial}$ is the initial solution, and X_{new} and $X_{mutated}$ are the new solution and mutated solution, respectively. Let P_t be the current parent population at generation t, crossover and mutation operations are performed on individuals from P_t to generate the offspring population Q_t. The initial solution and new solution are merged for population update, and the new population is selected as shown in *Equation 12*.

$$\begin{cases} P_{combined} = P_t \cup P_{offspring} \\ P_{t+1} = Select(P_{combined}) \end{cases} \quad (12)$$

In *Equation 12*, P_{t+1} represents the new population selected through non-dominated sorting and crowding distance. According to the optimisation formulas of NSGA-II, the algorithm progressively optimises the multi-objective solution set through selection, crossover and mutation operations [26]. The process of running NSGA-II to generate the Pareto front solutions is shown in *Figure 5*.

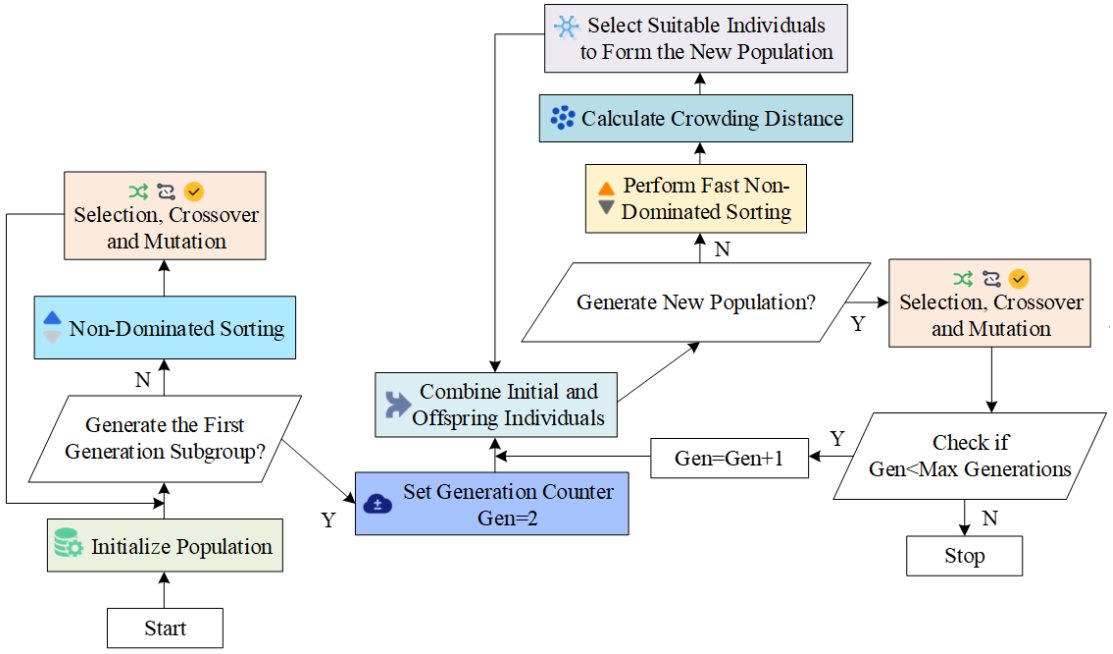

Figure 5 – Schematic diagram of the process of NSGA-II generating Pareto frontier solutions

Figure 5 demonstrates the process by which NSGA-II initiates with an initial population, generates the first generation of offspring, and sets the generation counter to 2. After merging the initial population with the offspring, quick non-dominated sorting and crowding distance calculation are performed to select suitable individuals for the new population. The next generation population is generated through selection, crossover and mutation operations. The current generation is then checked to see if the maximum number of generations has been reached. If not, the iteration continues until the termination condition is met and the final solution set is output. The entire process combines non-dominated sorting and crowding distance to ensure the quality and diversity of the solutions. Finally, the comprehensive objective is obtained through the dynamic combination of NSGA-II's Pareto front optimisation and TSVNS's local search, as shown in *Equation 13*.

$$Minimize\{Z_1, Z_2, -Z_3, Z_4\}, \quad \text{subject to constraints.} \quad (13)$$

In *Equation 13*, Z_1, Z_2, Z_3 and Z_4 represent minimising total transportation cost, minimising total transportation time, maximising freshness and minimising cold chain equipment energy consumption,

respectively. The constraints include capacity limits, time windows, temperature control, etc. Specifically, different objectives are set for the hybrid optimisation model, as shown in *Equation 14*.

$$\begin{cases} Z_1 = \sum_{k=1}^{K}\sum_{i=1}^{N}\sum_{j=1}^{N} c_{ij} \cdot x_{ijk} \\ Z_2 = \sum_{k=1}^{K}\sum_{i=1}^{N} t_{ik} \\ Z_3 = -\sum_{k=1}^{K}\sum_{i=1}^{N} \phi(t_{ik}) \cdot y_{ik} \\ Z_4 = \sum_{k=1}^{K}\sum_{i=1}^{N}\sum_{j=1}^{N} e_{ij} \cdot x_{ijk} \end{cases} \tag{14}$$

In *Equation 14*, c_{ij} represents the unit transportation cost from node i to node j, and x_{ijk} indicates whether vehicle k travels from i to j. t_{ik} represents the time at which the vehicle k reaches the node i. $\phi(t_{ik})$ is the function that reflects the impact of time on freshness, and y_{ik} indicates whether the goods at node i are delivered by vehicle k. e_{ij} is the unit energy consumption from node i to node j. The constraints are shown in *Equation 15*.

$$\begin{cases} \sum_{i=1}^{N} q_i \cdot y_{ik} \le Q_k, \quad \forall k \\ T_{\min} \le T_k \le T_{\max}, \quad \forall k \\ a_i \le t_{ik} \le b_i, \quad \forall i,k \\ \sum_{j}\sum_{k} x_{ijk} = 1, \quad \forall i \in Customers \\ \sum_{j=1}^{N} x_{ijk} = 1, \quad \forall i \in \text{CustomerSet} \end{cases} \tag{15}$$

In *Equation 15*, q_i represents the demand for goods at node i, and Q_k represents the capacity of vehicle k. T_k indicates the temperature of vehicle k, while $T_{\min}$ to $T_{\max}$ is the temperature range limit for agricultural products. $[a_i,b_i]$ represents the allowed arrival time window at node i. x_{ijk} indicates whether the logistics route from i to j will be used by vehicle k. This constraint ensures that each customer node i is visited exactly once by one vehicle. In NSGA-II, multiple objective functions are treated as independent optimisation directions, forming the Pareto front solution. The final integrated objective expression is $Minimize\{Z_1,Z_2,-Z_3,Z_4\}$, where each solution X represents a set of logistics route allocation decision variables $\{x_{ijk},y_{ik},t_{ik}\}$. Based on this, the NSGA-TSVNS hybrid optimisation model framework for agricultural product transportation is shown in *Figure 6*.

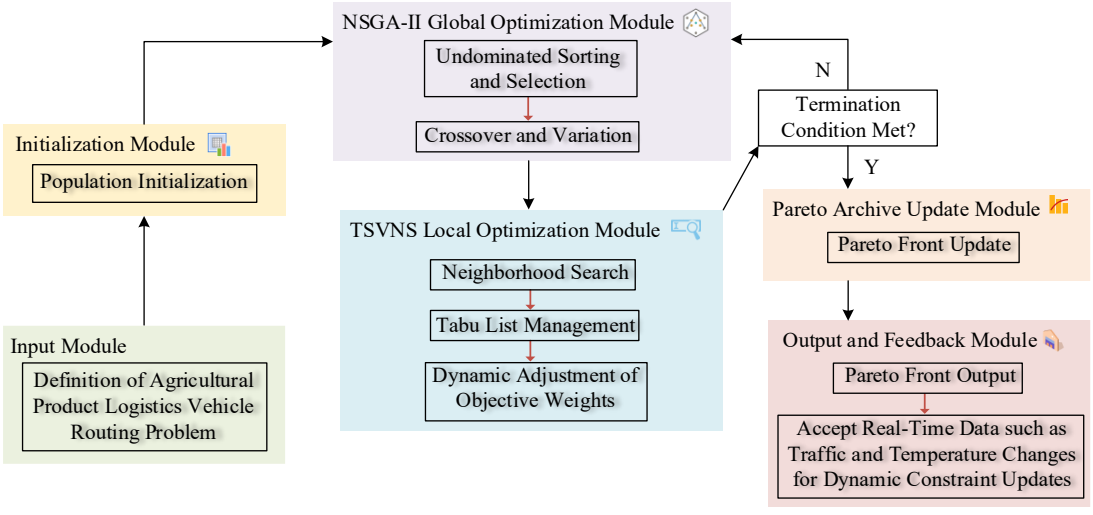

Figure 6 – NSGA-TSVNS model framework diagram

As shown in *Figure 6*, the NSGA-TSVNS model starts with the input module, defining the agricultural logistics vehicle routing problem and initialising the population. It then enters the NSGA-II global optimisation module, where optimisation solutions are generated through non-dominated sorting, individual selection, crossover and mutation. Next, it enters the TS-VNS local optimisation module, where the solution's local quality is improved through neighbourhood search, tabu list management and dynamic adjustment of objective weights. In the Pareto archive update module, the non-dominated solution set is updated, and finally, through the output and feedback module, the Pareto front solutions are output, while real-time data are used to dynamically update the constraints, forming an optimisation framework under dynamic environments.

3. RESULTS AND ANALYSIS

3.1 Performance validation of NSGA-TSVNS

To verify the performance of NSGA-TSVNS, the experimental environment was set up as follows. The hardware environment for the experiment included high-performance computing equipment, with a CPU of Intel Xeon E5-2680 v4, 2.4 GHz base frequency, 32 cores and 128 GB of memory. The software environment included the operating system Ubuntu 20.04 LTS, the programming language Python 3.8, and major libraries such as NumPy, Pandas, Matplotlib and specialised optimisation libraries like PyGMO and SciPy. In the cold chain logistics simulation experiment, the data source was divided into two categories: randomly generated example data and real cold chain logistics distribution data. The data sources included the classic Solomon dataset, BAM and PAM random examples. The number of cold chain delivery vehicles was set between 5 and 10, and the cold chain constraints included delivery time windows, temperature control ranges and refrigerated goods requirements. For the performance comparison experiment of NSGA-TSVNS, the comparison algorithms were set as TS and SA, with the objective function being total cost. The main evaluation metrics were convergence speed, total cost value, mean square error and mean absolute error. The adaptability to different example scales was also tested, with 10 runs performed and the average values recorded. The neighbourhood deconstruction performance of NSGA-TSVNS was first analysed, and the specific data are shown in *Table 1*.

Table 1 – Neighbourhood deconstruction performance analysis

Neighbourhood		**Solomon-12 × 2-W**	**20-5-1a-W**	**50-5-1a-W**	**100-10-1a-W**	**150-10-1a-W**
Cost all (thousand)		258.17	26074.00	35463.65	160565.39	225651.50
Delete the second-type neighbourhood	Cost1	262.15	26124.00	36126.00	161412.87	225684.32
	Gap (%)	1.62	0.17	2.56	0.54	0.02
Delete the second-type neighbourhood	Cost2	258.17	26135.00	36118.00	161438.16	2261.34
	Gap (%)	0.00	0.23	2.47	0.62	0.03
Delete the second-type neighbourhood	Cost3	258.17	26126.00	36121.00	060474.50	225654.34
	Gap (%)	0.00	0.15	2.51	0.56	0.01
Delete the second-type neighbourhood	Cost4	258.17	27576.00	38674.00	164065.24	230040.50
	Gap (%)	0.00	5.73	13.15	2.17	1.94

As shown in *Table 1*, the study conducted a detailed comparison of the performance of NSGA-TSVNS on different example scales. The total cost was the core metric, and the impact of progressively deleting the second-type neighbourhood on the optimisation performance was analysed. In the 50-5-1a-W example, the cost slightly increased after deleting the second-type neighbourhood, but the Gap remained within the controllable range of up to 2.56%. For larger-scale examples such as 100-10-1a-W and 150-10-1a-W, the Gap was less than 1% after deleting the second-type neighbourhood, and the cost increase was still small. To further validate the applicability of NSGA-TSVNS in complex environments and the model's fitting effectiveness, the study conducted an algorithm fitting degree validation for the objectives, and the results obtained are shown in *Figure 7*.

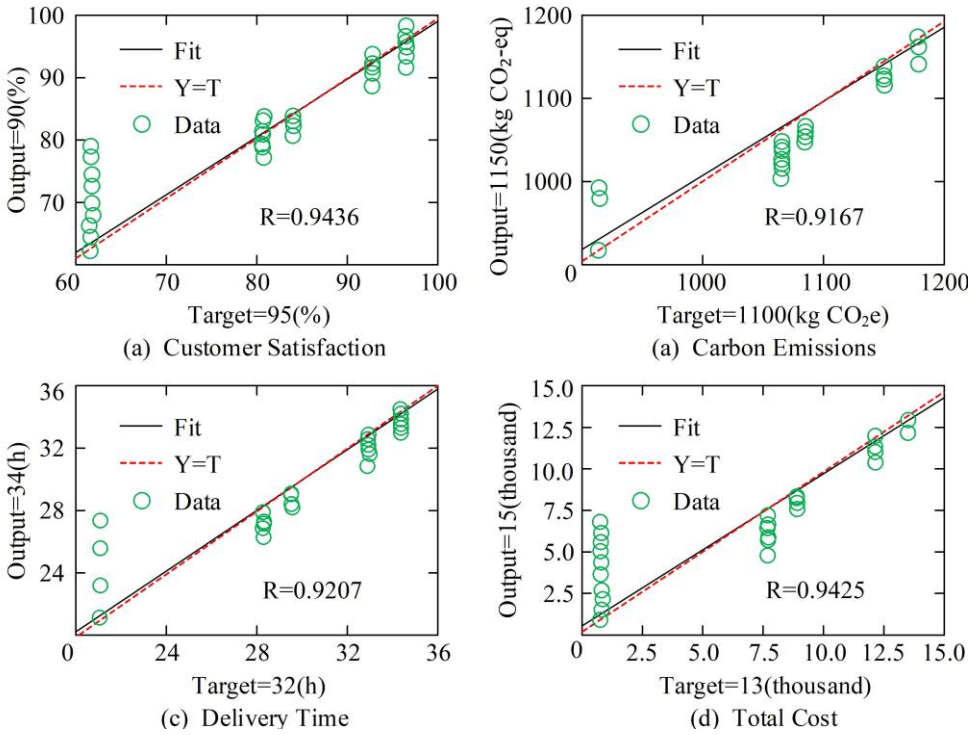

Figure 7 – Experimental results of applicability and fitting effects

In *Figure 7(a)*, the target value for customer satisfaction was 95%, with the output value being 90%. The actual data points were tightly and evenly distributed, and the fitting curve was close to the ideal line, indicating that the algorithm was able to optimise customer satisfaction well and approach the target. In *Figure 7(b)*, the target value for carbon emissions was 1,100 kg CO2e, with the output value being 1,150 kg CO2e. The data points were evenly distributed along both the fitting curve and the ideal line. In *Figure 7(c)*, the target value for delivery time was 32 hours, with the output value being 34 hours. The data points were tightly clustered around the fitting curve, demonstrating that NSGA-TSVNS showed strong stability in optimising time constraints. In *Figure 7(d)*, the target value for total cost was 13,000 yuan, with the output value being 15,000 yuan. The data points were evenly distributed around the fitting curve. Based on the analysis of the algorithm's fitting degree comparison, the optimisation performance and stability of NSGA-TSVNS in complex large-scale scenarios were validated through experimental results on large-scale examples. The results are shown in *Table 2*.

Table 2 – Optimised performance and stability experiment results

Computer power scale	Logistics cost			MSE (thousand)	MAE (thousand)
	NSGA-TSVNS	SA	TS		
1200	2.36	2.72	2.73	1.06	0.58
1250	2.45	2.78	2.78	1.28	0.62
1300	2.59	2.79	2.82	1.36	0.73
1350	2.62	2.84	2.93	1.47	0.84
1400	2.81	3.16	3.15	1.55	0.92
1450	2.84	3.16	3.19	1.63	1.01
1500	2.86	3.18	3.21	1.68	1.04
1550	2.97	3.26	3.43	1.77	1.13
1600	3.05	3.31	3.48	1.82	1.17
Average	2.73	3.02	3.08	1.51	0.89

As shown in *Table 2*, when the computational capacity was 1,200, the logistics cost for NSGA-TSVNS was 2,360 yuan, which was lower than both SA and TS. Additionally, its mean squared error (MSE) and mean absolute error (MAE) were 1,060 yuan and 580 yuan, respectively, indicating higher fitting accuracy. As the computational capacity gradually increased to 1,500, the MSE and MAE of the improved TSVNS were maintained at a relatively low level of 1,680 yuan and 1,040 yuan, further validating its robustness and efficiency in handling complex problems. Overall, NSGA-TSVNS achieved an average logistics cost of 2,655 yuan, which was significantly lower than SA's 2,963 yuan and TS's 2,978 yuan. At the same time, it demonstrated superior performance in terms of fitting error metrics. To illustrate the optimisation efficiency of the improved algorithm more intuitively in large-scale instances, the average cost convergence curves of each algorithm were compared. The performance evaluation results are shown in *Figure 8*.

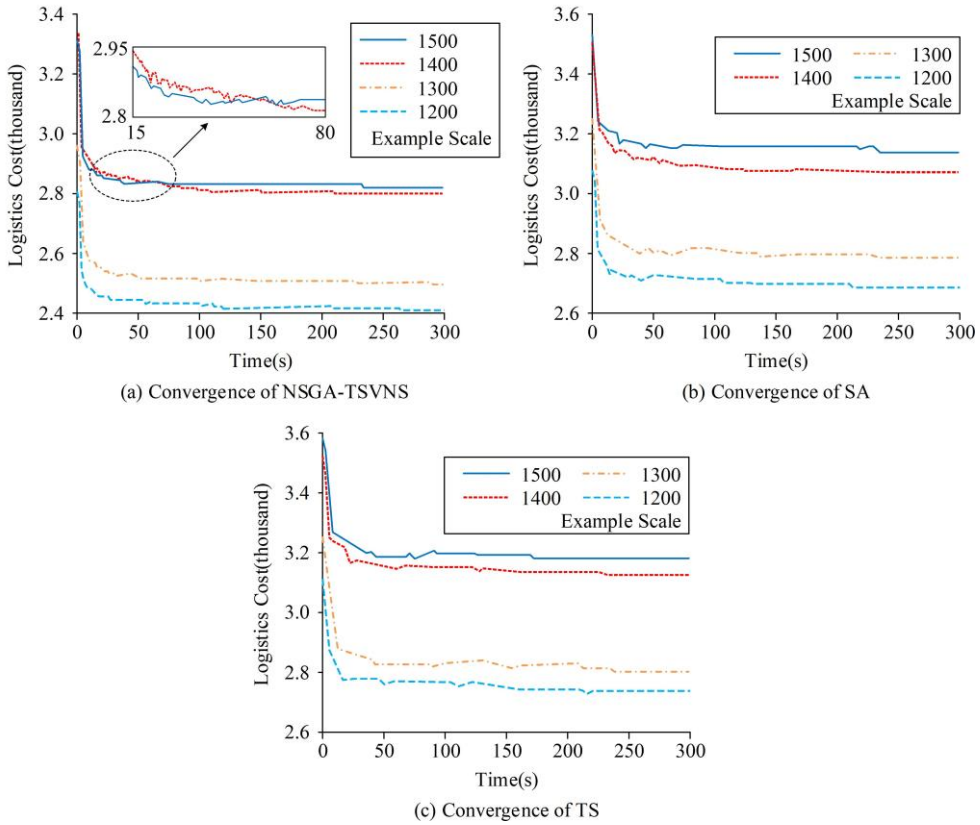

Figure 8 – Average cost experimental results

As shown in *Figure 8(a)*, TSVNS demonstrated faster convergence speed and lower final logistics costs across all example scales. In the initial phase, logistics costs rapidly decreased, with the main optimisation completed within 15 seconds, after which it entered a stable convergence phase. The final cost remained at a relatively low level, with the final cost for the 1,200-scale instance being 2,360 yuan. In contrast, *Figure 8(b)* shows that SA exhibited slower initial convergence speed under the same conditions, with a smaller decrease in costs. The final cost for the 1,500-scale instance was 3,180 yuan, which was much higher than the 2,860 yuan achieved by TSVNS. Additionally, SA's convergence curve showed greater fluctuations, indicating poorer solution stability. In *Figure 8(c)*, while TS's initial convergence speed was slightly faster than SA's, it also demonstrated higher final costs in the later convergence stages. The final cost for the 1,300-scale instance was 2,820 yuan, higher than NSGA-TSVNS's 2,590 yuan.

3.2 Performance analysis of NSGA-TSVNS logistics route optimisation model

Under the same experimental configuration, the study continued to analyse the performance of the NSGA-TSVNS model, targeting multi-objective optimisation problems. The optimisation objectives included operational cost, carbon emissions and customer satisfaction, while the evaluation metrics focused on the distribution quality, diversity and uniformity of the Pareto front solutions. The experimental environment was set with a temperature range from 5°C to 45°C, simulating low, medium and high temperature differences. The model was validated by comparing it with SA combined with a support vector machine (SVM) and VNS

combined with PSO. The total delivery cost, carbon emission cost and customer satisfaction performance were recorded during the optimisation process. Additionally, the convergence, coverage and uniformity of the solutions were analysed. The experimental results were presented using charts and a comparison of Pareto front solutions. To evaluate the optimisation effect of each algorithm on the average vehicle speed during congested periods, further comparisons were made regarding the adaptability and performance of different methods in a dynamic traffic environment. The results were obtained as shown in *Figure 9*.

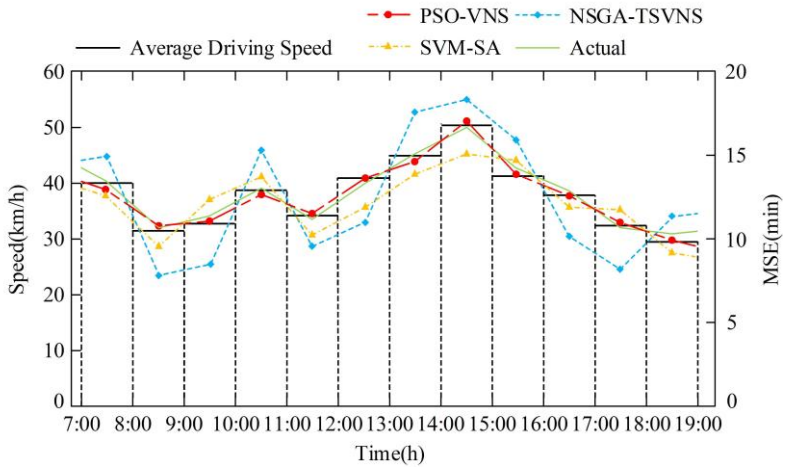

Figure 9 – Adaptation results in dynamic traffic environments

As shown in *Figure 9*, the actual data displayed the fluctuation trend of the driving speed throughout the day. After reaching a peak of 40 km/h at 7 AM, the speed gradually decreased, dropping to 31.4 km/h by 9 AM. The speed then peaked again at 50.2 km/h at 2 PM, followed by a slow decline to 29.5 km/h at 7 PM. In contrast, the NSGA-TSVNS model's fitted curve was much closer to the actual data. The MSE of the transportation time throughout the day was significantly lower than that of the other models. Notably, during periods with large speed fluctuations, such as the morning and afternoon rush hours, the NSGA-TSVNS model's fitted curve almost perfectly overlapped with the actual data. While the SVM-SA model and PSO-VNS model could reflect the overall trend, their fitting errors were larger, with the speed predictions at 9 AM and 2 PM deviating more from the actual values. The NSGA-TSVNS model, however, was able to capture the actual fluctuations more accurately. After analysing the vehicle speed optimisation during congested periods, the study compared the logistics route optimisation and task distribution balance through vehicle delivery route maps, as shown in *Figure 10*.

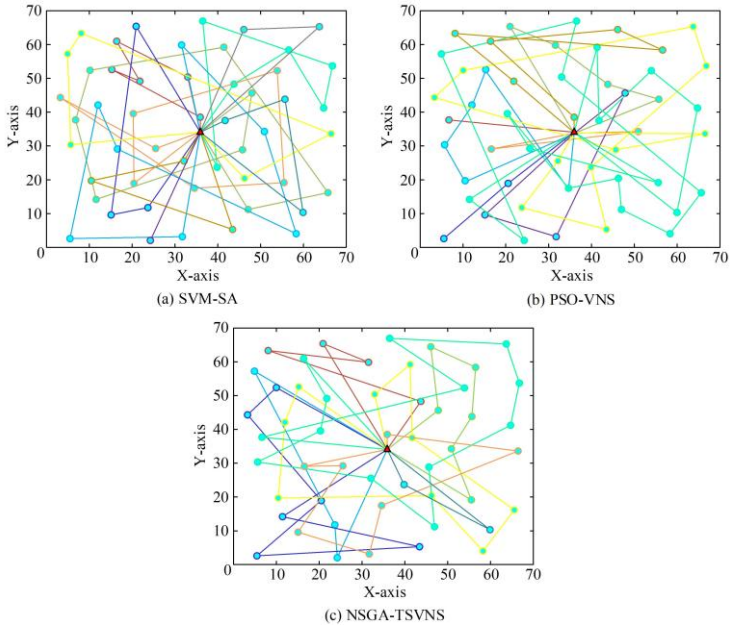

Figure 10 – Logistics route optimisation and tasking balance results

As shown in *Figure 10(a)*, the vehicle distribution logistics routes of the SVM-SA model exhibited a relatively complex overall distribution, with many route intersections. This potentially led to increased travel distance and decreased delivery efficiency. In *Figure 10(b)*, the logistics route planning of the PSO-VNS model showed some improvement in reducing route intersections; however, there were still cases where some vehicle routes were longer or node assignments were uneven. *Figure 10(c)* presents the logistics route planning of the NSGA-TSVNS model, where the number of route intersections was significantly reduced. The vehicle distribution within the delivery network was more uniform, and the task load and travel distance of each vehicle were more reasonable, reflecting a higher level of logistics route optimisation. Additionally, *Figure 10* revealed that the NSGA-TSVNS model designed 8 logistics routes, fewer than the 9 and 11 routes in the other two models. These results indicated that the logistics route planning of the NSGA-TSVNS model was more efficient. After comparing the vehicle delivery logistics route optimisation performance of each algorithm, the study further evaluated the solution distribution quality and balance in multi-objective optimisation through Pareto front analysis of the comprehensive optimal solutions. The comparison results of the models are shown in *Figure 11*.

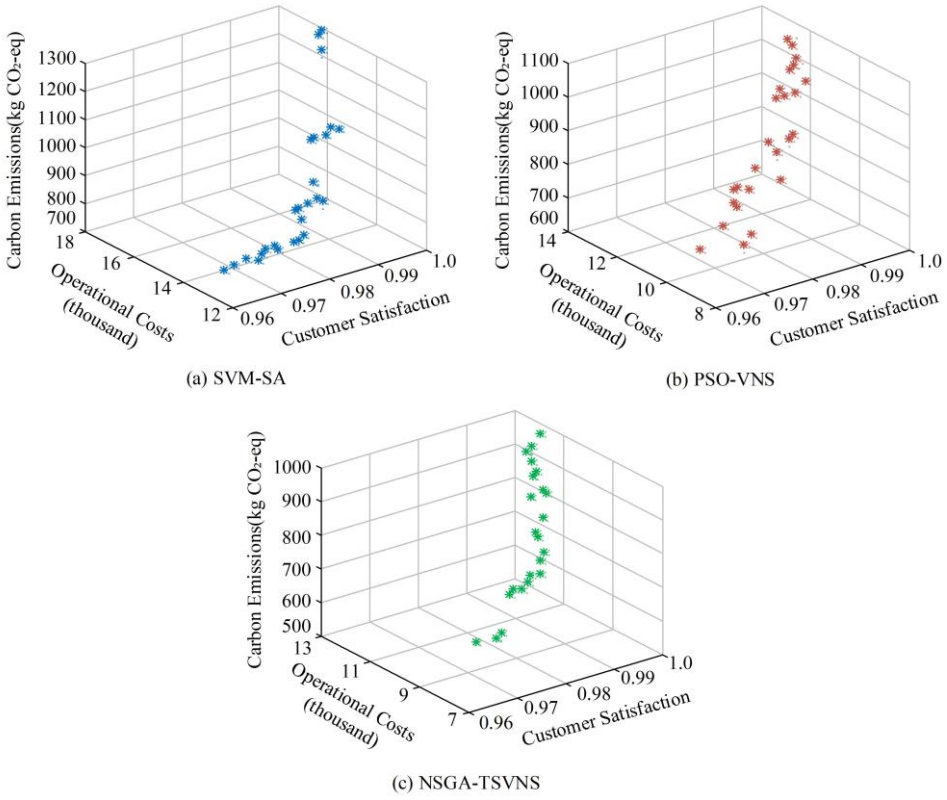

Figure 11 – Results on the distributional quality and equalisation performance of solutions

As shown in *Figure 11(a)*, the Pareto front distribution of the SVM-SA model was sparse and narrow, particularly in the solution space of low cost and high satisfaction, where the coverage was insufficient. In *Figure 11(b)*, the Pareto front of the PSO-VNS model had a broader distribution range, but the solution density in the low carbon emission and high customer satisfaction regions was low, with some areas still exhibiting uneven distribution. In *Figure 11(c)*, the Pareto front of the NSGA-TSVNS model showed the most uniform distribution and widest coverage in the three-dimensional space, especially in the solution space of low operating cost (7,000 to 11,000), low carbon emission (500 kg to 1,000 kg) and high customer satisfaction (0.96 to 0.99), where the distribution was dense. After analysing the Pareto front distribution of the comprehensive optimal solution, the study further compared the approximate Pareto solution set from 10 runs to verify the solution stability and convergence characteristics of the NSGA-TSVNS model in multiple optimisations. The solution quality performance is shown in *Figure 12*.

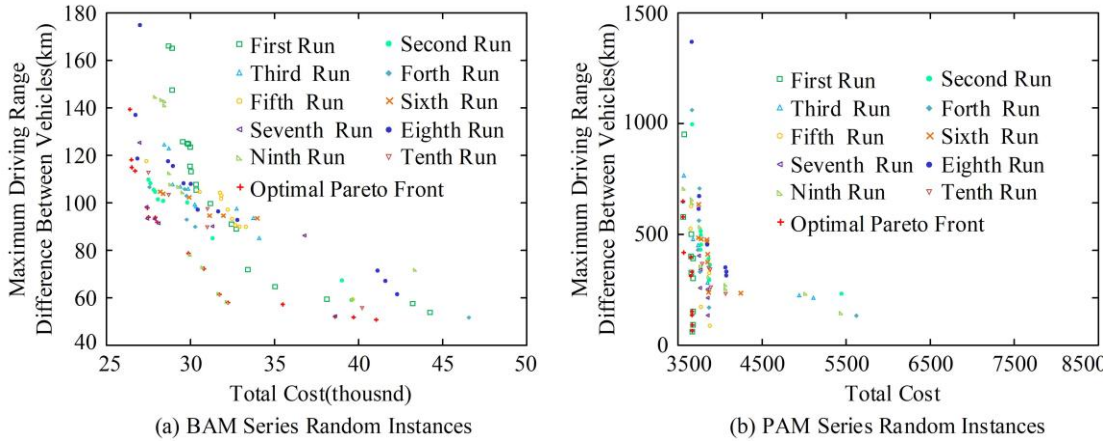

Figure 12 – Stability and convergence results for solutions

As shown in *Figure 12(a)*, with the increase in the number of runs, the solutions gradually approached the Pareto optimal frontier, particularly in the seventh, ninth and tenth runs, where the distribution of solutions became denser and closer to the optimal boundary. This indicated that NSGA-TSVNS exhibited good convergence and solution diversity in this case. In *Figure 12(b)*, with different numbers of runs, the solutions gradually approached the Pareto optimal frontier, and in the eighth and tenth runs, the distribution of the Pareto solution set became more comprehensive and uniform. Compared to earlier runs, the later solutions significantly reduced the total cost and maximum mileage difference, demonstrating the superior performance of NSGA-TSVNS in large-scale complex problems. Finally, the impact of different temperature difference environments on the optimisation performance and multi-objective balancing ability of the NSGA-TSVNS model was evaluated under comprehensive conditions, with the experimental results shown in *Table 3*.

Table 3 – Results of optimisation performance and multi-objective balancing ability

Temperature difference (°C)	Cost of goods damage	Refrigeration cost	Total carbon emissions (kg)	Carbon emission cost	Total distribution cost	Customer satisfaction (%)
5	365.32	104.80	747.86	526.11	6422.36	93.16
10	359.54	108.31	737.05	541.15	6493.51	90.35
15	370.66	116.52	858.34	597.92	6563.68	91.40
20	386.54	127.80	886.64	716.32	6643.71	90.76
25	397.94	127.69	896.95	723.02	6758.56	89.67
30	512.27	159.68	1037.40	749.32	6867.14	89.24
35	541.42	158.62	1090.75	765.96	6871.67	91.09
40	547.81	163.25	1225.48	783.89	7036.46	92.61
45	552.93	167.90	1247.56	820.91	7069.73	93.31

As shown in *Table 3*, the trends in various indicators under different temperature difference conditions were observed. With the increase in temperature difference, the cost of goods damage, refrigeration cost, total carbon emissions, carbon emission cost and total distribution cost generally showed an upward trend, while customer satisfaction fluctuated. As the temperature difference gradually increased from 5°C to 45°C, both the cost of goods damage and refrigeration cost showed a gradual increase. When the temperature difference was 5°C, the cost of goods damage was 365.32 yuan, and the refrigeration cost was 104.80 yuan. When the temperature difference increased to 45°C, the damage cost and refrigeration cost increased to 552.93 yuan and 167.90 yuan, respectively, indicating that high temperature difference conditions posed challenges to the economic efficiency of the cold chain logistics system. In terms of carbon emissions and carbon emission cost, both indicators also increased with the rise in temperature difference. The carbon emissions increased from 747.86 g at 5°C to 1247.56 g at 45°C, while the carbon emission cost increased from 526.11 yuan to 820.91 yuan, reflecting the environmental impact of the increased refrigeration demand.

4. DISCUSSION

The NSGA-TSVNS model proposed in the study demonstrated significant advantages in performance comparison experiments. In terms of cost control and the quality of the optimal frontier solutions, the NSGA-TSVNS model outperformed both the SVM-SA and PSO-VNS models. Especially in logistics route planning, the NSGA-TSVNS model designed 8 logistics routes, fewer than the 9 and 11 routes designed by the other two models. The optimised logistics routes had fewer crossings, and the distribution of vehicles in the delivery network was more uniform, resulting in higher vehicle logistics route delivery efficiency than the assembly VRP-D-MC proposed by Masmoudi M. A.'s team [27]. Multi-objective algorithms like NSGA-II typically perform excellently when dealing with traffic flow problems with multiple constraints and objectives, which is consistent with the findings of Kabiri N. N.'s team in their 2022 study [28]. Furthermore, the average vehicle speed calculated by NSGA-TSVNS matched the actual vehicle speed most closely, with an error within 1.5 km/h. This is because the algorithm took into account more factors related to traffic mobility and road conditions during its design, demonstrating its effectiveness and accuracy in simulating real traffic conditions. This aligns with the approach taken by Bai Q. et al., who used an improved NSGA-II to adapt to network complexity and time-varying traffic conditions to achieve Pareto optimal solutions [29].

NSGA-TSVNS not only offered a broader range of logistics route choices but also presented a more even and extensive distribution of Pareto frontier solutions. The Pareto front of each algorithm was displayed from the perspectives of operational cost, customer satisfaction and carbon emissions. NSGA-TSVNS, by integrating TS and VNS, provided strong local and global search capabilities. Its Pareto front was densely distributed in the solution space of low operational costs between 7,000 yuan and 11,000 yuan, low carbon emissions between 500 kg and 1,000 kg, and high customer satisfaction between 0.96 and 0.99, offering cost-effective and environmentally friendly solutions. Compared with Li D.'s team's DDNSGA-II model, the proposed model showed superior performance stability and adaptability under different environmental temperature variations [30]. This was because the model better considered the influence of environmental factors in the simulation and optimisation process, maintaining performance stability under changing conditions.

The contributions of this research were mainly in two aspects. First, a multi-objective optimisation NSGA-TSVNS model was proposed, which could handle multiple logistics optimisation objectives simultaneously. Second, the model effectively integrated environmental factors during the optimisation process. By optimising the cold chain logistics routes, the NSGA-TSVNS model helped maintain the appropriate temperature and environment for agricultural products during transportation, reducing product loss caused by delays or improper handling. These contributions provided valuable insights and references for improving agricultural logistics efficiency, reducing costs and supporting sustainable development.

5. CONCLUSION

In response to the difficulties of traditional methods in balancing solution quality and distribution in multi-objective optimisation, as well as the instability of optimisation results in dynamic environments, this study proposed a vehicle logistics route optimisation method based on NSGA-II and TSVNS. The method accurately modelled the constraints introduced by TSVNS and dynamically adjusted the tabu table and neighbourhood size using traffic and environmental data, thereby constructing the NSGA-TSVNS model. In terms of fitting effects across different indicators, TSVNS showed R-values close to 1, indicating that the method could stably and efficiently balance multiple objectives, while considering customer satisfaction, carbon emissions, delivery time and total cost. The results validated the scientific and practical applicability of the model. The findings show that the NSGA-TSVNS model can resolve multi-objective conflicts in cold chain logistics route optimisation and demonstrate high adaptability and stable solution quality in dynamic environments. Although the proposed model performed excellently, its computational complexity still needs further optimisation. Future improvements could focus on incorporating machine learning techniques to enhance the efficiency of generating initial solutions.

REFERENCE

[1] Yang C, et al. Edge-cloud blockchain and IoE-enabled quality management platform for perishable supply chain logistics. *IEEE Internet of Things Journal*. 2023;10(4):3264-3275. DOI: 10.1109/JIOT.2022.3142095.

[2] Cao Y, et al. Trajectory optimization for high-speed trains via a mixed integer linear programming approach. *IEEE Transactions on Intelligent Transportation Systems*. 2022;23(10):17666-17676. DOI: 10.1109/TITS.2022.3155628.

[3] Yao P, Wu K, Lou Y. Path planning for multiple unmanned surface vehicles using glasius bio-inspired neural network with hungarian algorithm. *IEEE Systems Journal*. 2023;17(3):3906-3917. DOI: 10.1109/JSYST.2022.3222357.

[4] Wang CN, et al. Scheduling flexible flow shop in labeling companies to minimize the makespan. *Computer Systems Science and Engineering*. 2022;40(1):17-36. DOI: 10.32604/CSSE.2022.016992.

[5] Hamza MA, et al. Energy-efficient routing using novel optimization with tabu techniques for wireless sensor network. *Computer Systems Science and Engineering*. 2023;45(2):1711-1726. DOI: 10.32604/csse.2023.031467.

[6] Azarkish M, Aghaeipour Y. A fuzzy bi-objective mathematical model for multi-depot electric vehicle location routing problem with time windows and simultaneous delivery and pick-up. *Asian Journal of Basic Science & Research*. 2022;4(2):1-3. DOI: 10.38177/AJBSR.2022.4201.

[7] Liu B, et al. Optimal routing of unmanned aerial vehicle for joint goods delivery and in-situ sensing. *IEEE Transactions on Intelligent Transportation Systems*. 2023;24(3):3594-3599. DOI: 10.1109/TITS.2022.3225269.

[8] Ranganathan V, et al. Re-inventing the food supply chain with IoT: a data-driven solution to reduce food loss. *IEEE Internet of Things Magazine*. 2022;5(1):41-47. DOI: 10.1109/IOTM.003.2200025.

[9] Liu Y, et al. Artificial intelligence in smart logistics cyber-physical systems: state-of-the-arts and potential applications. *IEEE Transactions on Industrial Cyber-Physical Systems*. 2023;1(5):1-20. DOI: 10.1109/TICPS.2023.3283230.

[10] Wu LJ, et al. Real environment-aware multisource data-associated cold chain logistics scheduling: a multiple population-based multiobjective ant colony system approach. *IEEE Transactions on Intelligent Transportation Systems*. 2022;23(12):23613-23627. DOI: 10.1109/TITS.2022.3203629.

[11] Saadi AA, et al. A hybrid improved manta ray foraging optimization with tabu search algorithm for solving the UAV placement problem in smart cities. *IEEE ACCESS*. 2023;11(5):24315-24342. DOI: 10.1109/ACCESS.2023.3255793.

[12] Zhang X, et al. Real-time scheduling of autonomous mining trucks via flow allocation-accelerated tabu search. *IEEE Transactions on Intelligent Vehicles*. 2022;7(3):466-479. DOI: 10.1109/TIV.2022.3166564.

[13] Hou Y, Wu Y, Han H. Multistate-constrained multiobjective differential evolution algorithm with variable neighborhood strategy. *IEEE Transactions on Cybernetics*. 2023;53(7):4459-4472. DOI: 10.1109/TCYB.2022.3189684.

[14] Song C, et al. An RFID-powered multisensing fusion industrial IoT system for food quality assessment and sensing. *IEEE Transactions on Industrial Informatics*. 2024;20(1):337-348. DOI: 10.1109/TII.2023.3262197.

[15] Müller FM, et al. GATeS: a hybrid algorithm based on genetic algorithm and tabu search for the direct marketing problem. *IEEE ACCESS*. 2024;12:20867-20884. DOI: 10.1109/ACCESS.2024.3353052.

[16] Abougharib A, Awad M, Ndiaye M. Remaining shelf-life estimation of fresh fruits and vegetables during transportation. *IEEE ACCESS*. 2023;11:8845-8859. DOI: 10.1109/ACCESS.2023.3239584.

[17] Wang W, Fang C, Liu T. Multiperiod unmanned aerial vehicles path planning with dynamic emergency priorities for geohazards monitoring. *IEEE Transactions on Industrial Informatics*. 2022;18(12):8851-8859. DOI: 10.1109/TII.2022.3153031.

[18] Yang X, Jiang H. Research on urban cold chain logistics path optimization considering multi-center and time-varying road networks. *IEEE ACCESS*. 2024;12(2):71331-71348. DOI: 10.1109/ACCESS.2024.3402833.

[19] Attenni G, et al. Drone-based delivery systems: a survey on route planning. *IEEE ACCESS*. 2023;11(12):123476-123504. DOI: 10.1109/ACCESS.2023.3329195.

[20] Zhang N, An Q, X. Wang. Loading method and routing optimizations of fresh products on multi-temperature joint distribution with limited flexible-size compartments. *IEEE ACCESS*. 2023;11(9):33261-33273. DOI: 10.1109/ACCESS.2023.3264211.

[21] Xie J, Chen J. Multiregional coverage path planning for multiple energy constrained UAVs. *IEEE Transactions on Intelligent Transportation Systems*. 2022;23(10):17366-17381. DOI: 10.1109/TITS.2022.3160402.

[22] Rashid SMM, Ali ME, Cheema MA. DeepAltTrip: Top-K alternative itineraries for trip recommendation. *IEEE Transactions on Intelligent Transportation Systems*. 2023;35(9):9433-9447. DOI: 10.1109/TKDE.2023.3239595.

[23] Wu G,et al. Collaborative truck-drone routing for contactless parcel delivery during the epidemic. *IEEE Transactions on Intelligent Transportation Systems*. 2022;23(12):25077-25091. DOI: 10.1109/TITS.2022.3181282.

[24] Yu Y, Xu Z, Zhao S. A two-stage algorithm based on 12 priority rules for the stochastic distributed resource-constrained multi-project scheduling problem with multi-skilled staff. *IEEE ACCESS*. 2023;11(3):29554-29565. DOI: 10.1109/ACCESS.2023.3261139.10.1109/TITS.2022.3181282.

[25] Chen X, et al. Robust optimization of energy-saving train trajectories under passenger load uncertainty based on p-NSGA-II. *IEEE Transactions on Transportation Electrification*. 2023;9(1):1826-1844. DOI: 10.1109/TTE.2022.3194698.

[26] Qiao K, et al. Evolutionary multitasking with global and local auxiliary tasks for constrained multi-objective optimization. *IEEE/CAA Journal of Automatica Sinica (JAS)*. 2023;10(10):1951-1964. DOI: 10.1109/JAS.2023.123336.

[27] Masmoudi MA, et al. Vehicle routing problems with drones equipped with multi-package payload compartments. *Transportation Research Part E: Logistics and Transportation Review*. 2022;164(24):102757. DOI: 10.1016/j.tre.2022.102757.

[28] Kabiri NN, Emami S, Safaei AS. Simulation-optimization approach for the multi-objective production anddistribution planning problem in the supply chain: using NSGA-II and Monte Carlo simulation. *Soft Computing*. 2022;26(17):8661-8687. DOI: 10.1007/s00500.022.07152.2.

[29] Bai Q, et al. Low-carbon VRP for cold chain logistics considering real-time traffic conditions in the road network. *Industrial Management & Data Systems*. 2022;122(2):521-543. DOI: 10.1108/IMDS.06.2020.0345.

[30] Li D, Li K. A multi-objective model for cold chain logistics considering customer satisfaction. *Alexandria Engineering Journal*. 2023;67(15):513-523. DOI: 10.1016/j.aej.2022.12.067.